Environmental risks assessment of kaolin mines and their brick products using monte carlo simulations

Article

Accepted Version

Orosun, M. M. ORCID: https://orcid.org/0000-0002-0236-3345, Usikalu, M. R., Oyewumi, K. J., Onumejor, C. A., Ajibola, T. B., Valipour, M. and Tibbett, M. ORCID: https://orcid.org/0000-0003-0143-2190 (2022) Environmental risks assessment of kaolin mines and their brick products using monte carlo simulations. Earth Systems and Environment, 6. pp. 157-174. ISSN 2509-9426 doi: 10.1007/s41748-021-00266-x Available at https://centaur.reading.ac.uk/101127/

It is advisable to refer to the publisher's version if you intend to cite from the work. See Guidance on citing.

To link to this article DOI: http://dx.doi.org/10.1007/s41748-021-00266-x

Publisher: Springer

All outputs in CentAUR are protected by Intellectual Property Rights law, including copyright law. Copyright and IPR is retained by the creators or other copyright holders. Terms and conditions for use of this material are defined in the End User Agreement.

www.reading.ac.uk/centaur

CentAUR

Central Archive at the University of Reading

Reading's research outputs online

Environmental Risks Assessment of Kaolin Mines and their Brick Products using Monte Carlo Simulations

[1]Muyiwa Michael Orosun (0000-0002-0236-3345), [2]Mojisola Rachael Usikalu, [1]Kayode John Oyewumi, [2]Charity Adaeze Onumejor, [1]Taiye Benjamin Ajibola, [3]Mohammad Valipour and [4]Mark Tibbett

[1]Department of Physics, University of Ilorin, Ilorin, Kwara State, Nigeria
[2]Department of Physics, Covenant University, Ota, Ogun State, Nigeria.
[3]Department of Civil and Environmental Engineering and Water Resources Research Center, University of Hawaii at Manoa, Honolulu, HI, 96822, USA.
[4]Department of Sustainable Land Management & Soil Research Centre, School of Agriculture Policy and Development, University of Reading, Whiteknights, Reading, RG6 6AR, England.
Corresponding author: *muyiwaorosun@yahoo.com*

Abstract

This study aimed to assess the radiological health implications to humans due to the use of kaolin from kaolin mines in Nigeria. A calibrated RS-125 spectrometer was used *in-situ* to monitor the activities of ^{40}K, ^{238}U, ^{232}Th and dose-rate of kaolin minefields in Ilorin-south and Ilorin-west, Nigeria. The *in-situ* monitoring and measurements were done in 90 locations selected at random in the study areas. The *in-situ* measurements were consolidated via laboratory analysis of 48 samples of Kaolin bricks using lead-shielded NaI(Tl) detector. The estimated average values for all radiological hazard parameters for the in-situ measurements of Ilorin-west are higher than that of Ilorin-south minefield. However, the opposite was the case with the laboratory analysis of the bricks. This apparent conundrum was due to the higher values of ^{238}U observed in the samples of bricks from Ilorin-south. Additionally, the measured activities of the primordial radionuclides in the Kaolin bricks from both mines are lower than the on-site measurements. This was attributed to the contribution from other terrestrial materials on-site. The 5th, 50th, and 95th percentiles of the cumulative probabilities for the excess lifetime cancer risk using the Monte Carlo simulation are 167.00×10^{-6}, 281.00×10^{-6}, 414.00×10^{-6} for Ilorin-west (*in-situ*), 104.00×10^{-6}, 232.00×10^{-6}, 392.00×10^{-6} for Ilorin-south (*in-situ*), 706.00×10^{-6}, $1,250.00\times10^{-6}$, $1,900.00\times10^{-6}$ for Ilorin-west (Lab), and 742.00×10^{-6}, $1,480.00\times10^{-6}$, $2,460.00\times10^{-6}$ for Ilorin-south (Lab), respectively. Therefore, the cancer risks are within the acceptable limits for both mining sites. This study is useful in developing radiation risk assessment models for decision makers in different fields of environmental sciences.

Keywords: Kaolin, Gamma ray spectrometry, Natural radionuclides, Radiological hazards, Environmental risk assessment.

Article Highlights:

- The laboratory measured activity concentrations of ^{40}K, ^{238}U and ^{232}Th in all the locations are lower than their respective *in-situ* measurements.
- The estimated average values for all radiological hazard parameters for the *in-situ* measurements of Ilorin-west are higher than that of Ilorin-south minefield. However, the opposite was the case with the laboratory analysis of the bricks.
- The cancer risk assessment using the Monte Carlo simulations reveals values that are mostly within the recommended permissive limits

1. Introduction

Kaolin, also known as china clay, typically contains about 85 percent of kaolinite that is formed through weathering of the mother rock under favorable conditions. Additionally, kaolin typically contains small amounts of mica, feldspar, illite and quartz. Due to its good physical, mineralogical and chemical characteristics, Kaolin is extensively utilized as a raw material in production of ceramics, cements, paints, refractory bricks, tiles, papers, drugs, toothpastes, fabrics, rubbers and plastics (Turhan, 2009). The Raw Materials Research and Development Council (RMRDC) of Nigeria has drawn attention to the numerous benefits of kaolin production in Nigeria and put the estimated annual national demand at over 360,000 tones (Dailytrust, 2018; Leadership, 2018). This demand is usually met by locally mined Kaolin. In Nigeria, because bricks prepared from Kaolin are cheap, easy to produce and have good geotechnical properties, they are widely used as raw materials for building and construction (Dailytrust, 2018; Leadership, 2018).

All raw materials used for building and construction resulting from weathering of mineral rocks, such as limestone, laterite and kaolin, often contain considerable level of radioelements like ^{238}U, ^{232}Th, their daughter elements and the non-series ^{40}K. These radionuclides are usually inherited from the parent rock during pedogenesis. Since the presence of these naturally occurring radioelements in the building and construction materials contributes to radiation exposure, information about the level of these natural radionuclides in building materials becomes very important in assessing the possible radiological hazards to human health. Knowledge about the concentration of these radionuclides is also very important in developing standards and rules that will help to check and manage the use of these mineral soils as building materials (Janković et al., 2018; Turhan, 2009).

In Nigeria, the activities of ^{238}U, ^{234}Th and their progenies together with the non-series ^{40}K in different materials used for building and construction from diverse locations of the country have been reported (Ajibola et al., 2021; Orosun et al., 2019, 2020; Omeje et al., 2018; Adagunodo et al., 2018; Isinkaye et al., 2015; Usikalu et al., 2014, 2016, 2019; Ajayi et al., 2012; Ademola et al., 2008; Farai and Ademola, 2001). Unfortunately, beside the work of Olusola et al. in 2013, where they investigated the geochemical and mineralogy of the Kaolin, no work has been carried out in Kwara on the assessment of natural radionuclides despite the growing level of Kaolin mining and usage for construction in Nigeria. Cancer incidence in Ilorin could be attributed to over exposure to elevated level of background ionizing radiation from the use of mined mineral soils such as the kaolin for building purposes because epidemological studies have shown a strong correlation between cancer incidence and exposure to enhanced level of ionizing radiation (IARC, 1988). Hence, the aim of this present work is to assess the radiological risk at the mine sites and relate this to the human health risk of kaolin bricks exported from the mine for use in construction.

2. Material and Methods

2.1. Study Area

The study areas are Fufu village in Ilorin-south and Akerebiata area of Ilorin-west in Kwara State, Nigeria. The latitudes/Longitudes description of the location are 8º20' N and 8º50' N and 4º25' E and 4º65'E as shown in figures 1a, 1b and 1c. Ilorin town is known to have sedimentary rock base, and has both primary/secondary laterites and alluvial deposits (Orosun et al., 2020a; Ajadi et al., 2016; Oyegun, 1985). The collection of basement-complex rocks in the study area resulted in the numerous ferruginous groups of soils of high percentage of clay content. The soils originate from Igneous and metamorphic rocks which is typical of basement complex that is almost 95%. The metamorphic rocks found in the area constituents majorly of banded gnesiss, biotite gnesiss, granitic gnesiss and quartzite augitegnesiss, while the constituent of intrusive rocks are vein quartz and pegmatite (Orosun et al., 2020a; Ajadi et al., 2016; Kayode et al, 2015; Oyegun, 1985). More information on the geology of the study area had been reported by (Orosun et al., 2020a, 2020b, 2021; Ajadi et al., 2016; Kayode et al, 2015; Oyegun, 1985).

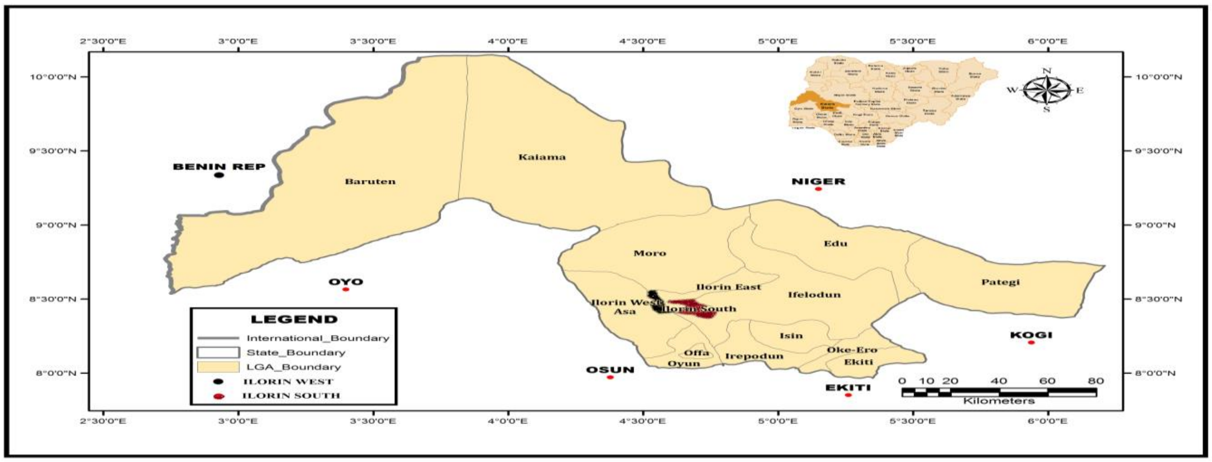

Fig. 1a. Map of Kwara state showing the study areas.

Map data © 2019 CNES/Airbus, Maxar Technologies

Fig. 1b. Base map of Ilorin-west Kaolin mining field showing the sampling locations.

Map data © 2019 CNES/Airbus, Maxar Technologies

Fig. 1c. Base map of Ilorin-south Kaolin mining field showing the sampling locations.

2.2. Field Survey

In-situ quantitative measurements of ^{40}K, ^{232}Th, ^{238}U activities and the radiation dose exposures at the two biggest Kaolin mines in Kwara state was carried out using gamma spectrometer (Super SPEC RS-125, Canadian Geophysical Institute). This instrument employed a large 2.0 x 2.0 NaI crystal which offered superior unified design with a large detector with good sensitivity. Activity determination of the radionuclide heads were made at approximately1m above the topsoil in keeping with previous studies (Adagunodo et al., 2018, Orosun et al., 2019). The RS-125 gamma spectrometer was calibrated by manufacturer and initialized for use in Nigeria. Calibration was completed on 1 x 1 m test pads that stored 5min spectra accumulation on potassium, uranium and thorium pads and 10 min accumulation on the background pad. The equipment has a very high degree of accuracy with probable errors in measurement of about ± 5 % (Radiation Solution Inc., 2015; Oyeyemi et al., 2017; Adagunodo et al., 2018, Orosun et al., 2019). Further details of the spectrometry methods can be found in previous studies (Radiation Solution Inc., 2015; Oyeyemi et al., 2017; Adagunodo et al., 2018, Orosun et al., 2019).

At the Ilorin-south mine site, 50 spatially random sample points were recorded together with their standard deviations. At the Ilorin-west mine site, 40 randomly selected sample points were assessed. For more accuracy, the readings were repeated 5 times at each sample location. The geographical coordinates and elevations of each of the sampling points were recorded using a GPSMAP78 global positioning system.

2.3. Sample preparation and Gamma-Ray Spectrometry

Twenty-four (24) samples each were collected randomly from blocks/bricks made with the kaolin soil from the mining sites. This brings the total samples to 48. The samples were collected in a rubber test containers of about 10 ml each using a plastic trowel. These samples were sent to the laboratory where they were screened to remove macroscopic traces of glass, rubber, hair, animal and plant matter to ensure that the materials to be analysed are free from non-mineral contaminants. The samples were ground using agate mortar and sieved through a 1 mm sieve mesh and stored in labelled plastic containers (Marinelli cylindrical beakers) and kept for 40 days to ensure secular radioactive equilibrium before the Gamma-Ray spectrometry. The detector that was used for the radioactivity measurements is a 3 x 3 inch lead-shielded NaI(Tl) detector produced by Princeton Gamma Tech. USA. The NaI(Tl) detector is coupled to Gamma Spectacular (GS-2000-Pro) Multichannel Analyzer (MCA) through a preamplifier. The linearity of the detector was tested and found to be satisfactory. RSS8 gamma source set, Spectrum Techniques LLC, USA, were used for the energy resolution calibration. The spectral data from the standard gamma sources were obtained with an energy range of 511 – 2,620 KeV (Orosun et al., 2020; Isinkaye, 2018). The detection efficiency calibration was carried out using standard reference materials IAEA-RGK-1, IAEA-RGU-1, and IAEA-RGTh-1 consisting of known activities of ^{40}K, ^{238}U and ^{232}Th. The resolution of the detector at 662 keV of ^{137}Cs is 8% full width at half maximum (FWHM). Each sealed sample were placed on the shielded NaI(Tl) detector and counted for 18000 seconds. The empty control container was also counted for the same counting time of 18000 seconds to determine the background distribution spectrum. Canberra S100 gamma ray acquisition software was used for the gamma counting process after which the spectra information was retrieved and the analysis was carried out using the comparative method i.e. The specific radioactivity "C_x" in the sample and the corresponding specific radioactivity "Cs" in the standard material are related by;

$$C_x = C_s \frac{M_s A_x}{M_x A_s} \quad 1$$

where, C_x = concentration of specific radioactivity in the sample, C_s = specific activity concentration of the standard, M_s = mass of the standard, M_x = mass of the sample, A_s = area of the standard and A_x = area of the sample.

This data analysis software subtracted a linear net background distribution from the corresponding net peaks area for a particular radionuclide in the spectra of the samples. The activity concentration of ^{214}Bi (determined from its 1764.5 keV γ-ray peak) was selected to provide an estimate of ^{238}U in the samples, while 2614.7 keV of ^{208}Tl was chosen as an indicator of ^{232}Th. ^{40}K was determined by measuring the 1460 KeV γ-rays emitted during its decay (Orosun et al., 2020; Isinkaye, 2018; Joel et al., 2018a; Omeje et al., 2020). The minimum detectable activity for ^{40}K, ^{238}U and ^{232}Th was 0.0255, 0.00737 and 0.00737 Bqkg^{-1}, respectively, for the NaI(Tl) detector used in this study.

3. Results and Discussion

3.1. In situ Activity concentration

The statistical summary of the *in situ* measured activity concentrations of ^{238}U, ^{232}Th, ^{40}K and the gamma dose rate (*DR*) together with their standard deviation (*SD*) for Kaolin mines in Ilorin-west and Ilorin-south are shown in Tables 1 and 2 respectively. From Table 1, the highest values of the activity concentration of ^{40}K, ^{238}U, ^{232}Th and *DR* for Ilorin-west are 782.50 ± 27.04, 69.16 ± 3.62, 66.99 ± 5.72 $Bqkg^{-1}$ and 81.92 ± 7.16 $nGyh^{-1}$, respectively, while their corresponding lowest values are 156.50 ± 2.10, 1.24 ± 0.12, 22.33 ± 1.60 $Bqkg^{-1}$ and 45.92 ± 2.14 $nGyh^{-1}$, respectively. From Tables 2, the highest values of the activity concentration of ^{40}K, ^{238}U, ^{232}Th and *DR* for Ilorin-south are 532.10 ± 30.17, 132.15 ± 13.22, 69.02 ± 3.01 $Bqkg^{-1}$ and 88.30 ± 6.92 $nGyh^{-1}$, respectively, while their corresponding lowest values are 31.30 ± 1.15, 1.24 ± 0.01, 5.28 ± 1.02 $Bqkg^{-1}$ and 13.90 ± 1.13 $nGyh^{-1}$, respectively. The mean values of the measured activity concentration of ^{40}K, ^{238}U, ^{232}Th and *DR* for the Ilorin-west (Akerebiata) Kaolin mine field were found to be 492.19, 35.63, 44.07 $Bqkg^{-1}$ and 63.28 $nGyh^{-1}$ respectively. While the mean values for the measured activity concentrations of ^{40}K, ^{238}U, ^{232}Th and *DR* for the Ilorin-south (Fufu) were 263.55, 52.24, 31.29 $Bqkg^{-1}$ and 54.71 $nGyh^{-1}$, respectively. The mean values of ^{40}K, ^{232}Th and *DR* for the Kaolin mine site in Ilorin-west are higher than that of the estimated mean values for Ilorin-south. In contrast, the mean value of ^{238}U for Ilorin-west is less than the estimated mean value for Ilorin-south.

According to the International Commission on Radiological Protection (ICRP, 1991), International Atomic Energy Agency (IAEA, 1996) and United Nations Scientific Committee on the Effects of Atomic Radiation (UNSCEAR, 2000) report, the recommended values for general populace for exposure to ^{40}K, ^{238}U, ^{232}Th and *DR* are given as 420.00, 32.00, 45.00 $Bqkg^{-1}$ and 59.00 $nGyh^{-1}$, respectively. The estimated mean values of ^{40}K, ^{238}U and *DR* for the Kaolin mine site in Ilorin-west were higher than the recommended global average values. These values are cause for concern since considerable increase in the concentration of the radionuclides causes increase in the level of the background radiation which may render the mineral soil unfit for use in building and construction purposes. Even though the average value of ^{232}Th for the Ilorin-west mine field is less than the recommended global average of 45.00 $Bqkg^{-1}$, it was observed that the 50% (20 out of 40) measured values were higher than the reported global average values. For the Kaolin mine field in Ilorin-south, only the estimated mean value of ^{238}U is higher than its corresponding recommended limit. The mean values of ^{40}K, ^{232}Th and DR were lower than their global averages.

To further study the distribution of these measured radionuclides and the gamma dose rate, Surfer™ version 15 was used to plot 3D maps for the two mine fields (Figures 2 to 9). Two colors (green and red) were adopted to reflect areas with values within and greater than the recommended limits. Red colour which is commonly used to signify danger, represent areas with values higher than the recommended average while green field represents areas within the recommended limits. The 3D maps revealed that the Ilorin-west mine field is blessed with ^{40}K and ^{238}U which in turn contributes to the outdoor gamma dose rate. The enhancement of the dose rate caused by these radionuclides is evident in Figure 5 wherein, more red fields are seen. The 3D maps also revealed that the Ilorin-south mine field is rich in ^{238}U (Figure 7).

Comparing the mean values of ^{40}K, ^{238}U, ^{232}Th and DR for the two studied fields with selected studies from literatures, as shown in Table 4, it was revealed that these average values obtained in this study compare well with the values reported for Ifonyintedo (Kaolin, Nigeria) (Adagunodo et al., 2018), as well as Asa (Granite, Nigeria) (Orosun et al., 2019 and 2020), and Ilorin (Laterite, Nigeria) (Orosun et al., 2020b).

Table 1. Descriptive Statistics of the in-situ measured activities of ^{40}K, ^{238}U, ^{232}Th and DR of Kaolin mining field in Akerebiata area of Ilorin-west LGA.

Stat	***DR* *(nGyh^{-1})***	***^{40}K* *(Bqkg^{-1})***	***^{238}U* *(Bqkg^{-1})***	***^{232}Th* *(Bqkg^{-1})***
Minimum	45.92±2.30	156.50±23.10	1.24±0.40	22.33±3.10
Maximum	81.92±11.20	782.50±72.20	69.16±11.40	66.99±7.20
Median	62.90±1.70	438.20±35.70	35.82±6.20	45.07±1.80
Mode	N/A	657.30±21.10	35.82±2.10	29.23±2.30
Range	36.00	626.00	67.92	44.66
Sum	2531.12	19687.70	1425.30	1762.86
Mean ± SD	63.28±10.48	492.19±156.90	35.63±17.66	44.07±13.94
Standard Error	1.66	24.81	2.79	2.20
Standard Deviation (SD)	10.48	156.90	17.66	13.94
Sample Variance	109.82	24617.22	311.80	194.29
Kurtosis	-0.98	-0.89	-0.32	-1.22
Skewness	0.12	0.03	-0.08	0.14
Coefficient of Variation	16.56	31.88	49.56	31.63
Count	40.00	40.00	40.00	40.00

Table 2 Descriptive Statistics of the in-situ measured activities of ^{40}K, ^{238}U, ^{232}Th and DR of Kaolin mining field in Fufu area of Ilorin-south LGA.

Stat	***DR* *(nGyh^{-1})***	***^{40}K* *(Bqkg^{-1})***	***^{238}U* *(Bqkg^{-1})***	***^{232}Th* *(Bqkg^{-1})***
Minimum	13.90±2.30	31.30±4.20	1.24±0.40	5.28±1.30
Maximum	88.30±21.20	532.10±150.40	132.10±11.30	69.00±13.20
Median	54.80±12.10	250.40±48.70	49.40±3.20	29.40±4.30
Mode	54.80±12.10	156.50±23.20	38.29±3.60	29.20±4.10
Range	74.40	500.80	130.86	63.72
Sum	2735.30	13177.30	2612.02	1562.74
Mean ± SD	54.71±16.68	263.55±145.18	52.24±27.01	31.25±15.60
Standard Error	2.36	20.53	3.82	2.21
Standard Deviation (SD)	16.68	145.18	27.01	15.60
Sample Variance	278.22	21076.93	729.32	243.21
Kurtosis	0.05	-0.97	0.71	0.35
Skewness	-0.18	0.26	0.73	0.60
Coefficient of Variation	30.49	55.09	51.70	49.90
Count	50.00	50.00	50.00	50.00

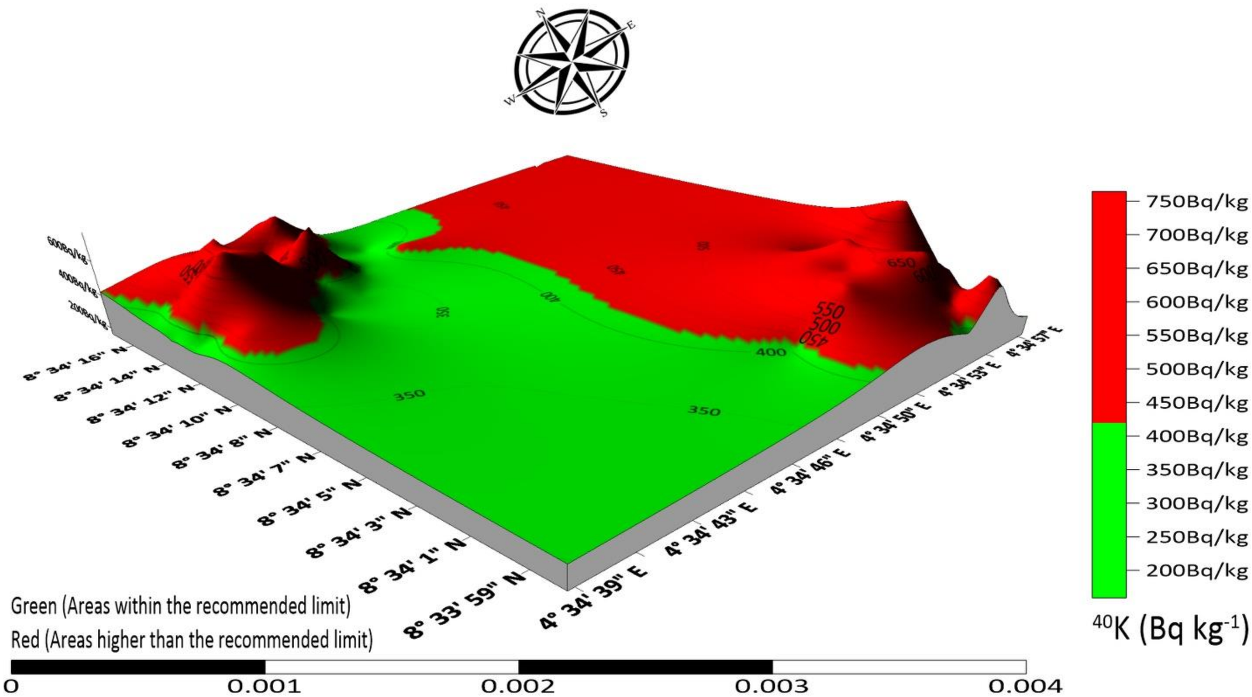

Fig. 2. Isopotassium 3D map of Ilorin-west Kaolin mining field (Red colour represents areas with values higher than the recommended global average value of 450.00 Bqkg^{-1} while the green field represents areas within the recommended limits).

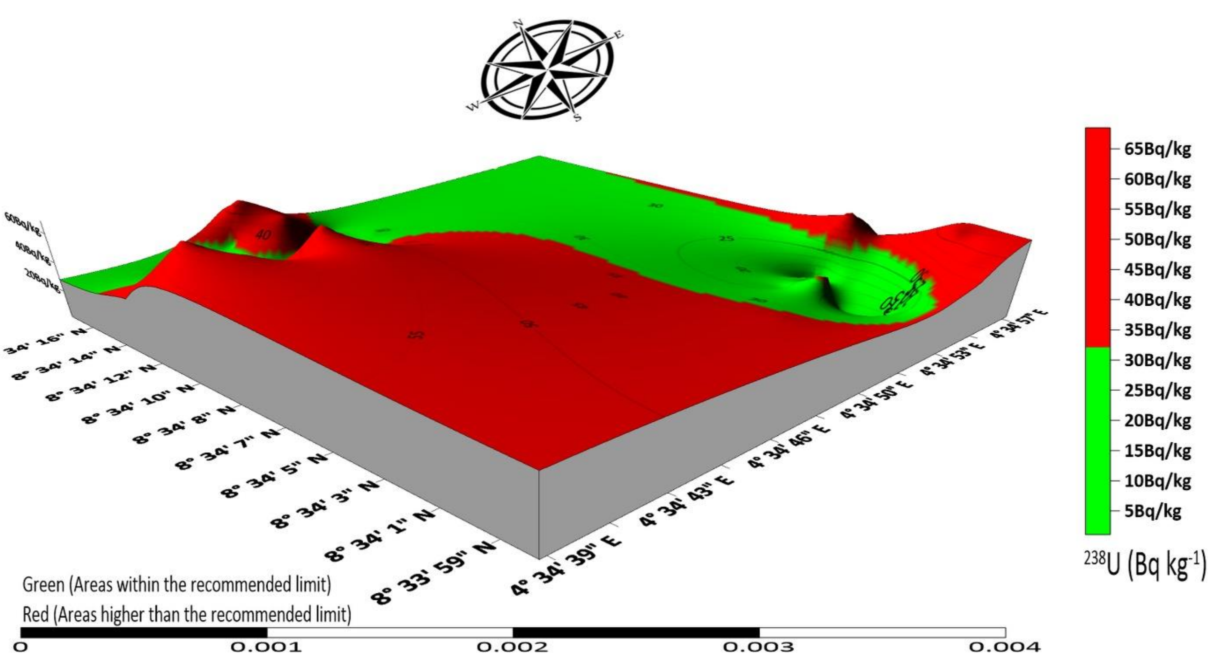

Fig. 3. Isouranium 3D map of Ilorin-west Kaolin mining field (Red colour represents areas with values higher than the recommended global average value of 32.00 Bqkg^{-1} while the green field represents areas within the recommended limits).

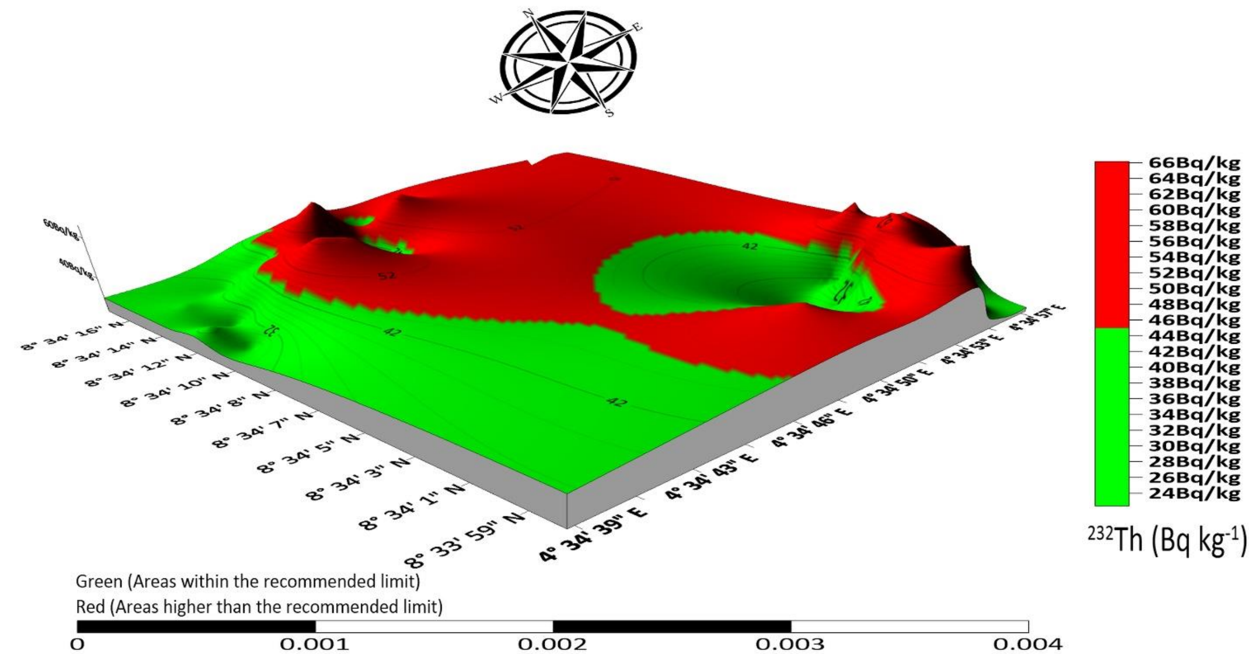

Fig. 4. Isothorium 3D map of Ilorin-west Kaolin mining field (Red colour represents areas with values higher than the recommended global average value of 45.00 Bqkg^{-1} while the green field represents areas within the recommended limits).

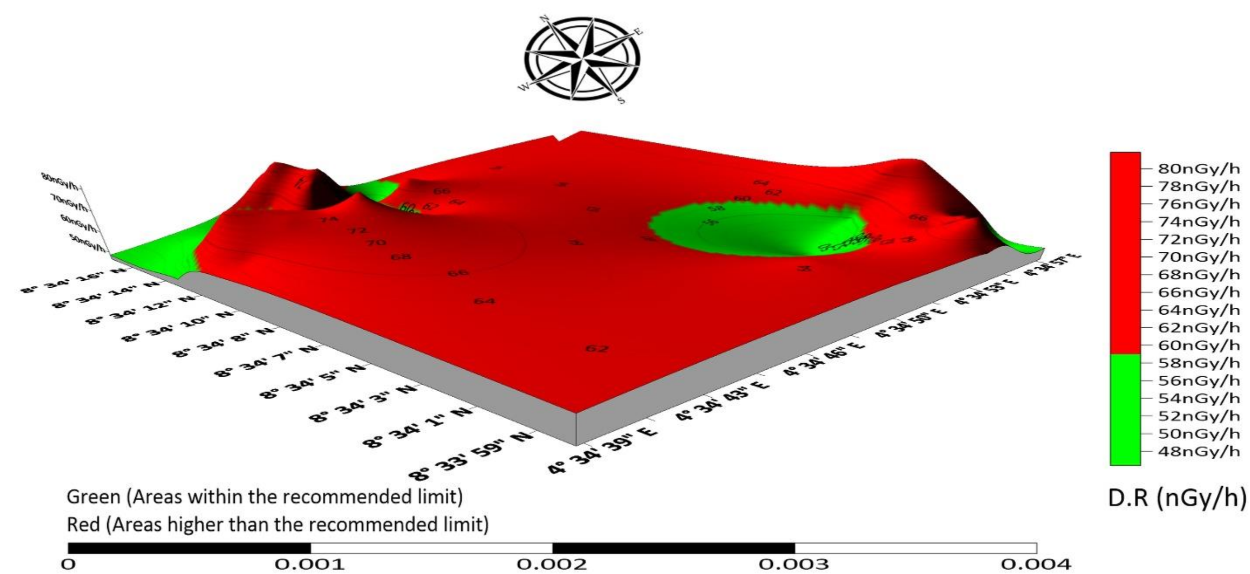

Fig. 5. Isodoserate 3D map of Ilorin-west Kaolin mining field (Red colour represents areas with values higher than the recommended global average value of 59.00 nGyh^{-1} while the green field represents areas within the recommended limits).

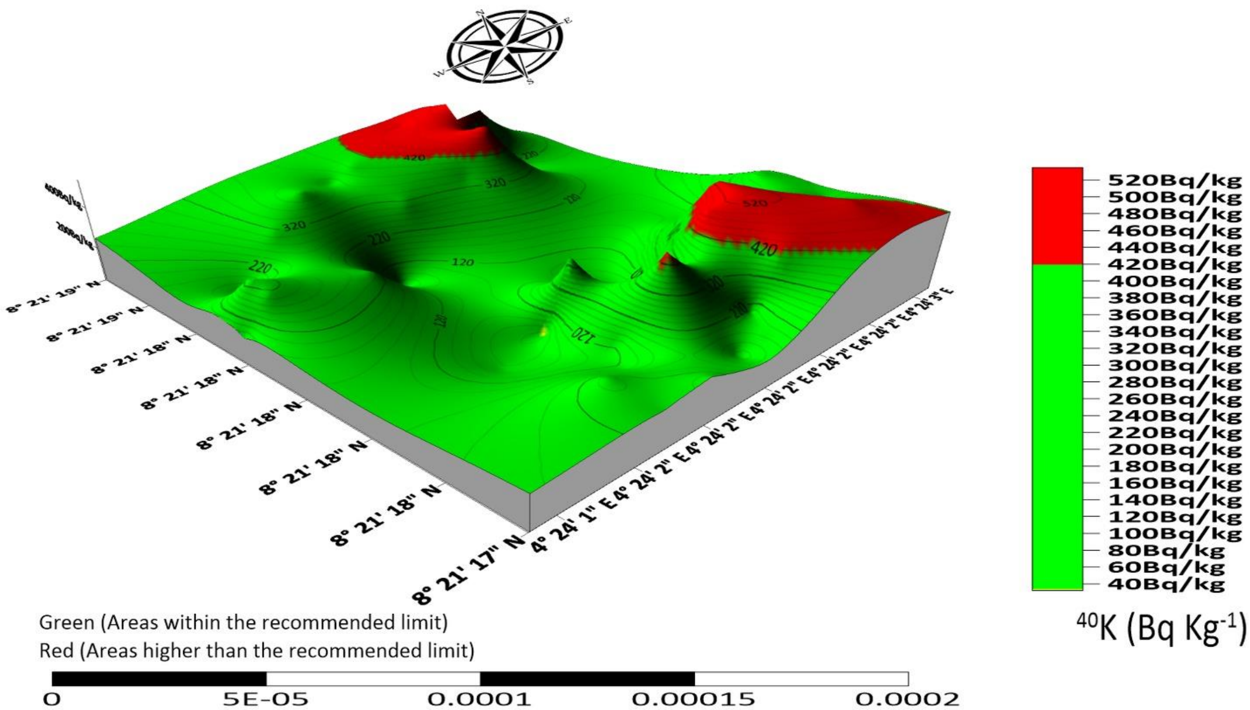

Fig. 6. Isopotassium 3D map of Ilorin-south Kaolin mining field (Red colour represents areas with values higher than the recommended global average value of 450.00 Bq/kg while the green field represents areas within the recommended limits).

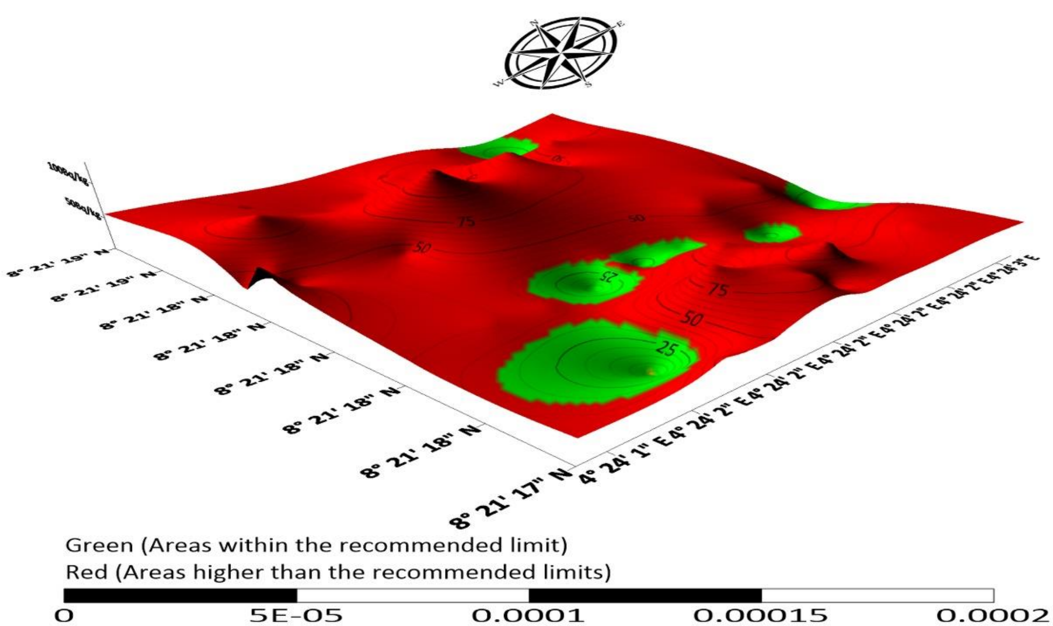

Fig. 7. Isouranium 3D map of Ilorin-south Kaolin mining field (Red colour represents areas with values higher than the recommended global average value of 32 Bq/kg while the green field represents areas within the recommended limits).

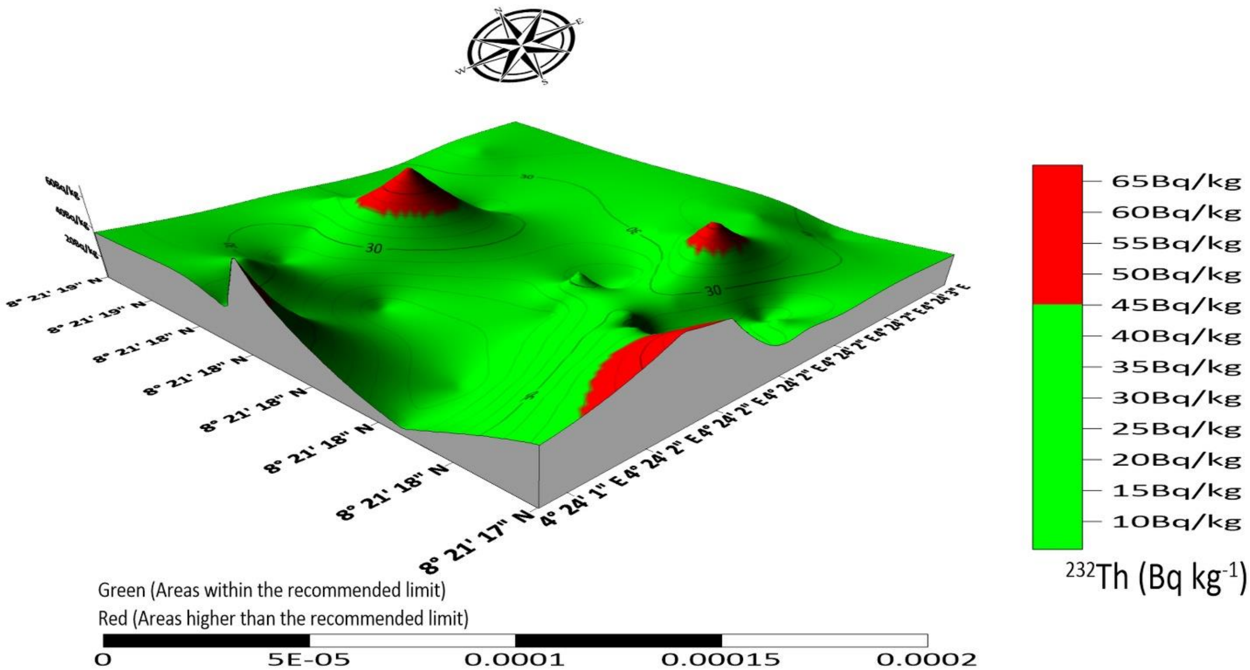

Fig. 8. Isothorium 3D map of Ilorin-south Kaolin mining field (Red colour represents areas with values higher than the recommended global average value of 45.00 Bq/kg while the green field represents areas within the recommended limits).

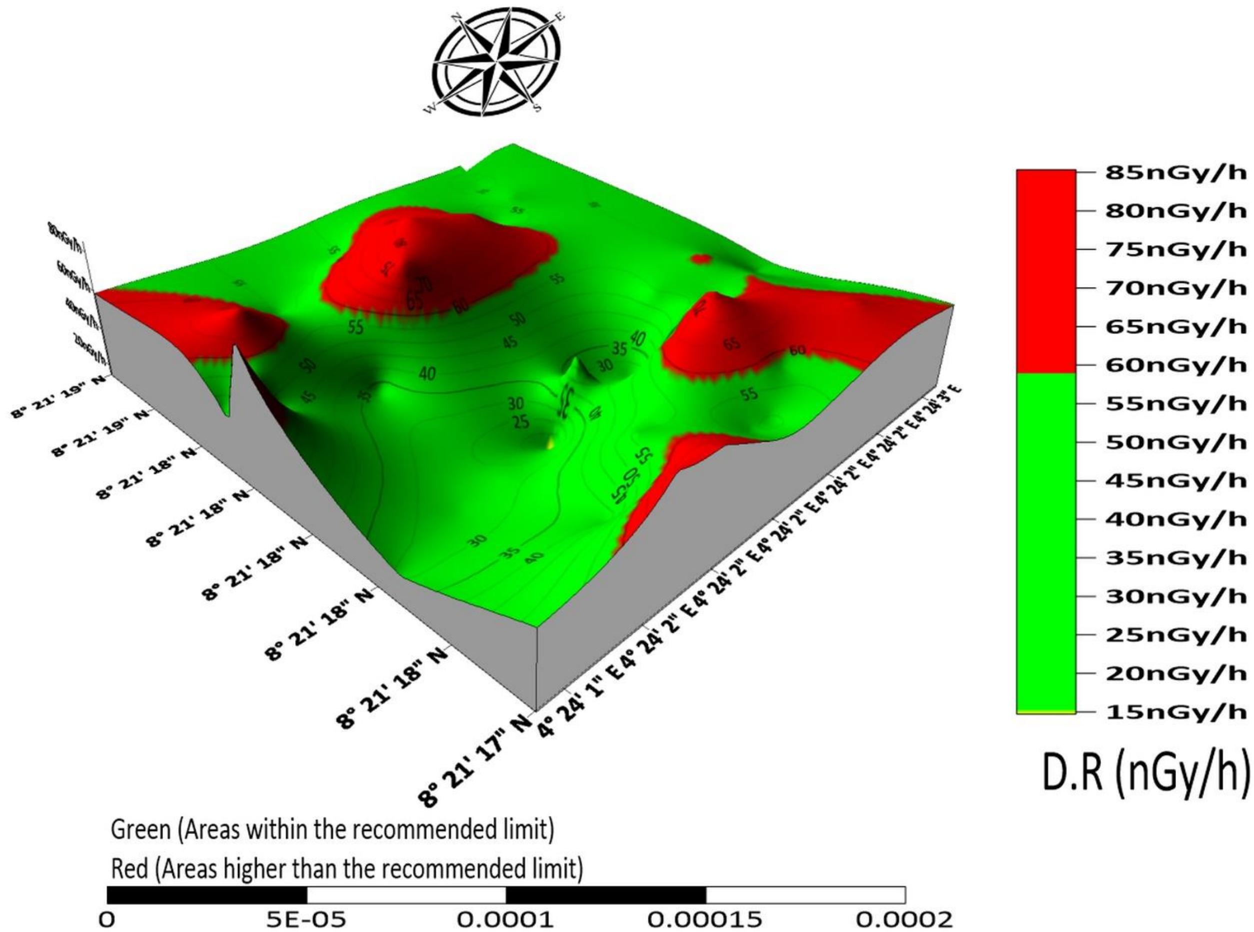

Fig. 9. Isodoserate 3D map of Ilorin-south Kaolin mining field (Red colour represents areas with values higher than the recommended global average value of 59.00 nGy/h while the green field represents areas within the recommended limits).

3.2. Radioactivity content in the selected soil samples from the study areas

Since *in situ* measurements are insufficient for quantitative determination of activity concentrations, we consolidated our measurements with laboratory analyses. The summary of the radioactivity content in the sampled blocks/bricks made with soils collected from the mining sites is presented in Table 3. The activity concentration of ^{40}K appeared to be far higher than that of ^{232}Th and ^{238}U. This tendency was observed at all study locations. The results for all radionuclide heads studied (i.e. ^{238}U, ^{232}Th and ^{40}K) were skewed moderately; this means that the spread is moderately asymmetric, because most of the measure of the asymmetry of their probability distribution is in the range of -2 and +2 about their means.

The mean values of the measured activity concentration of ^{40}K, ^{238}U and ^{232}Th for the Ilorin-west (Akerebiata) Kaolin minefield were 189.28, 23.80 and 32.40 $Bqkg^{-1}$ respectively. While the mean values for the measured activity concentrations of ^{40}K, ^{238}U and ^{232}Th for the Ilorin-south (Fufu) are 92.34, 42.73 and 27.06 $Bqkg^{-1}$ respectively. The mean values of ^{40}K and ^{232}Th for the Kaolin minefield in Ilorin-west are higher than that of the estimated mean values for Ilorin-south. However, the mean value of ^{238}U for Ilorin-west is less than (about half) the estimated mean value for Ilorin-south. This is in accord with the *in situ* measurements. Interestingly, all the *in situ* measurements were higher than their respective measured activity concentrations of ^{40}K, ^{238}U and ^{232}Th in all the locations. This may be attributed to contribution by other terrestrial materials on-site to the gamma ray detection during the course of *in situ* measurements.

Table 3 Statistical summary of the measured activity concentrations of ^{40}K, ^{238}U, ^{232}Th in samples collected from mining site using 3 x 3 inch NaI[Tl].

SAMPLE LOCATION	**SAMPLE STAT**	**^{40}K ($Bqkg^{-1}$)**	**^{238}U($Bqkg^{-1}$)**	**^{232}Th($Bqkg^{-1}$)**
	MIN	118.23 ± 13.20	12.57 ± 3.50	22.56 ± 6.20
	MAX	299.40 ± 91.10	36.82 ± 8.20	48.38 ± 9.10
ILN-WEST	SKEW	1.52	0.65	1.60
	MEAN±SD	189.28 ± 96.70	23.80 ± 6.22	32.40 ± 13.96
	MIN	48.36 ± 4.70	10.80 ± 2.20	2.56 ± 1.20
ILN-SOUTH	MAX	129.40 ± 67.20	86.82 ± 25.10	54.38 ± 13.70
	SKEW	-0.74	1.26	0.48
	MEAN±SD	92.34 ± 19.96	42.73 ± 9.44	27.06 ± 6.02
GLOBAL AVERAGE		**420.00**	**32.00**	**45.00**

Table 4 Comparison of the mean activity concentration and dose rate with other studies.

Material	^{238}U (Bq kg^{-1})	^{232}Th (Bq kg^{-1})	^{40}K (Bq kg^{-1})	*Dose rate (nGy h^{-1})*	Location	References
Soil	19.16	48.56	1146.88	89.6	India	Chandrasekaran et al. (2014).
Kaolin	82	94.8	463.6	117.7	Turkey	(Turhan, 2009).
Clay	39.3	49.6	569.5	74.1	Turkey	(Turhan, 2009).
Floor ceramic	101.22	87.53	304.57	213.98	Iraq	(Amana, 2017).
Wall ceramic	102.12	70.9	328.6	178.4	Iraq	(Amana, 2017).
Kaolin	964.7	251.6	58.9	58.1	Eqypt	(El-Dine et al., 2004).
Phosphogypsum	206.8	99.1	15.1	154.6	Brazil	(Mazzilli and Saueia, 1999).
Kaolin	38.2	65.1	93.9	59.6	Nigeria (Ifonyintedo)	(Adagunodo et al., 2018).
Granite	11.51	15.42	441.06	32.72	Nigeria	(Orosun et al., 2020).
Granite	18.15	42.86	570.91	60.11	Nigeria	(Orosun et al., 2019).
Laterite	43.89	38.79	81.38	46.44	Nigeria	(Orosun et al., 2020b).
Kaolin	35.63	44.07	492.19	63.28	Nigeria (Ilorin-west)	Present study (*In situ*)
Kaolin	52.24	31.29	263.55	54.71	Nigeria (Ilorin-south)	Present study (*In situ*)
Kaolin	23.8	32.4	189.28	38.32	Nigeria (Ilorin-west)	Present study
Kaolin	42.73	27.06	92.34	39.87	Nigeria (Ilorin-south)	Present study
Soil and Rock	32	45	420	59	Global Average	(UNSCEAR, 2000).

3.3. Evaluation of the Radiological Impact Parameters

3.3.1. Radium Equivalent Activity (Ra_{eq})

The radiation exposure has been defined in terms of radium equivalent activity (Ra_{eq}) in $Bqkg^{-1}$ to evaluate the specific activity of substance having differing amounts of ^{238}U, ^{232}Th *and* ^{40}K because the distribution of these radionuclides in the Kaolin is not uniform. The assumption is that 0.7 $Bqkg^{-1}$ of ^{232}Th, 1 $Bqkg^{-1}$ of ^{238}U and 13 $Bqkg^{-1}$ of ^{40}K produces equal radiation dose rates. This permits the use of a solitary index to represent the gamma dose due to different mixture of ^{238}U, ^{232}Th and ^{40}K in the Kaolin. The Ra_{eq} was calculated using equation (2) (UNSCEAR, 2000; Orosun et al. 2018, 2018a):

$$Ra_{eq} = C_U + 1.43C_{Th} + 0.077C_K \quad 2$$

C_U, C_{Th} and C_K are the activity concentrations in *Bqkg*$^{-1}$ for ^{238}U, ^{232}Th and ^{40}K respectively. The recommended average value for it is 370 *Bqkg*$^{-1}$ (UNSCEAR, 2000; ICRP, 1991; IAEA, 1996). The maximum, minimum and mean values for the Ra_{eq} obtained for *in situ* measurements are 175.45, 98.10 and 136.55 *Bqkg*$^{-1}$ respectively, for the Ilorin-west Kaolin minefield and 193.49, 32.61 and 117.28 *Bqkg*$^{-1}$ respectively, for the Ilorin-south Kaolin mine field. For the laboratory gamma spectrometry results, the Ra_{eq} values ranges between 117.57 - 53.93 *Bqkg*$^{-1}$ with mean value of 84.70 *Bqkg*$^{-1}$ for Ilorin-west location, and ranges between 168.31 - 41.87 *Bqkg*$^{-1}$, with a mean value of 88.54 *Bqkg*$^{-1}$. All the measured values (both laboratory and *in situ*) for the two mine sites are less than the recommended limit.

3.3.2. Radiation Hazard Indices

The internal radiation hazards (H_{int}) and the external radiation hazard (H_{ext}) were calculated using equations (3) and (4);

$$H_{int} = \left(\frac{C_U}{185}\right) + \left(\frac{C_{Th}}{259}\right) + \left(\frac{C_K}{4810}\right) \quad 3$$

$$H_{ext} = \left(\frac{C_U}{370}\right) + \left(\frac{C_{Th}}{259}\right) + \left(\frac{C_K}{4810}\right) \quad 4$$

C_U, C_{Th} and C_K are defined in equation (2).

Both H_{int} and H_{ext} have to be less than 1 for it to be considered as low radiation hazard. Natural radionuclides in mineral soils produce external radiation to which the general populaces are exposed. The mean values of H_{int} and H_{ext} for the Ilorin-west are 0.47 and 0.37 for *in situ* measurements and 0.29 & 0.23 for bricks samples lab gamma spectrometry respectively. While for Ilorin-south, the mean values were found to be 0.46 and 0.32 for *in situ* and 0.36 & 0.24 respectively. These values are within the permissible value of unity.

3.3.3. Absorbed Dose Rate

Generally, at about 1m above the ground level, naturally occurring radionuclides are assumed to have a uniform distribution. The outdoor dose rate (DR) at about 1 m above the ground was obtained *in situ* using the RS-125 gamma spectrometer and indoor absorbed dose (for bricks used for building purposes) was calculated using equation 5 (Omeje et al., 2021; Akinyose et al., 2018; Adagunodo et al., 2018; Orosun et al., 2017; UNSCEAR, 2000).

The Kaolin from both Ilorin-west and Ilorin-south are used basically for building purposes. It implies that, the indoor radiation dose rate in a particular building with wall thickness of about 20 *cm* and room size 2.8×4 × 5 *m*, is given by:

$$D_i(nGy\,h^{-1}) = 0.92C_u + 1.1C_{Th} + 0.08C_K \qquad 5$$

The *in situ* mean values of D_o (DR) and the D_i for the Ilorin-west is 63.28 and 72.67 $nGyh^{-1}$ respectively, while for Ilorin-south, the mean values were found to be 54.71±16.68 and 76.47 ± 18.24 $nGyh^{-1}$ respectively (see Table 5). As expected, these mean values of D_o for Ilorin-west are higher than that of Ilorin-south mine field. However, the opposite was the case with D_i. This apparent conundrum was primarily due to the high values of ^{238}U observed in the samples of bricks from Ilorin-south (i.e. the mean concentration of ^{238}U of Ilorin-south is almost twice the mean value obtained for bricks samples from Ilorin-west). The mean value of D_i for both Ilorin-west and Ilorin-south are less than the recommended limit of 84.00 $nGyh^{-1}$ given by (UNSCEAR, 2000). This follows that indoor gamma radiation exposure risk is relatively low for the Kaolin soils, but the publics might not be considered safe from indoor exposure to ionizing radiation, since no amount of radiation is safe for stochastic effects.

3.3.4. Annual Effective Dose (AED)

The annual effective dose received indoor and outdoor by a member of the general public was calculated using dose rates. Dose conversion factor of 0.7 $SvGy^{-1}$ and occupancy factor for outdoor and indoor as 0.2 and 0.8 were used (UNSCEAR, 2000; Isinkaye et al., 2015; Omeje et al., 2021).

$$AED_{out}\,(mSvy^{-1}) = D_o \times 8760 \times 0.7 \times 0.2 \times 10^{-6} \qquad 6$$

$$AED_{in}\,(mSvy^{-1}) = D_i \times 8760 \times 0.7 \times 0.8 \times 10^{-6} \qquad 7$$

The mean values for the AED_{out} and AED_{in} for Ilorin-west are 0.08 and 0.36 $mSv\ y^{-1}$ respectively, while that of Ilorin-south are 0.07 and 0.38 $mSv\ y^{-1}$ respectively. While the mean AED_{out} for Ilorin-west is above the global limits provided by UNSCEAR (2000), the mean AED_{out} for Ilorin-south is approximately equal to the recommended limit of 0.07 $mSvy^{-1}$. The mean values of the AED_{in} for both Ilorin-west and south are lower than the recommended limit of 0.41 $mSvy^{-1}$.

3.3.5. Excess Lifetime Cancer Risk (ELCR)

The Excess Lifetime Cancer Risk (*ELCR*) was calculated using equation (8):

$$ELCR = AED \times DL \times RF \qquad 8$$

AED is the indoor Annual Equivalent Dose Equivalent, *DL* represents the mean human lifespan (given as 70 years) and RF is the stochastic Risk Factor in Sv^{-1}. The fatal cancer risk (*RF*) per Sievert is given as 0.05 set by ICRP for the public (UNSCEAR, 2000; Orosun et al., 2018). All the values estimated for the *ELCR* (i.e. for both Ilorin-west and south) were below the recommended limits of 3.75 x 10^{-3}.

3.3.6. Annual Gonadal Equivalent Dose (AGED)

An increase in annual gonadal equivalent dose (*AGED*) has been reported to increase the likelihood of developing leukemia that can be fatal to humans. The annual gonadal equivalent dose (*AGED*) for the residents using the bricks for building and construction was calculated using equation (9) (UNSCEAR, 2000; Orosun et al., 2018; Usikalu et al., 2017):

$$\text{AGED } (\mu Sv\, y^{-1})\ C = 3.09\ C_U + 4.18\ C_{Th} + 0.314\ C_K \qquad 9$$

The *AGED* mean values estimated for the residents using the Kaolin bricks for building were evaluated and found to be only slightly lower than the recommended limit of 0.3 $mSv\, y^{-1}$ (see last column of Table 6). However, the estimated *AGEDs* for the *in situ* measurements were higher than the recommended 0.3 $mSvy^{-1}$. These high values obtained for *AGED* increase our fear over the use of these kaolin soils for building and construction purposes.

3.3.7. Representative Level Index (RLI)

The *RLI* was estimated using equation 10 (UNSCEAR, 2000; Orosun et al., 2018):

$$RLI = \frac{C_u}{150} + \frac{C_{Th}}{100} + \frac{C_k}{1500} \qquad \leq 1 \qquad 10$$

The mean *RLI* for the kaolin mine fields were estimated and to be 1.01 and 0.84 or *in situ* measurements, and 0.61 & 0.62 for the lab results respectively for Ilorin-west and south. The mean *RLI* for Ilorin-west is greater than the recommended limit of unity while that of Ilorin-south is close to 1. This shows that care should be taken in the use of these kaolin soils for building purposes.

Tables 5 and 6 shows the summary of the evaluated hazard risk parameters for the measured activity concentrations. The contributions of the measured radionuclides (^{40}K, ^{238}U and ^{232}Th) to the radiological hazard parameters were displayed in Figures 10 and 11. It was observed that ^{40}K and ^{234}Th were the main contributors to the radiological hazards for Ilorin-west while ^{238}U is the chief contributor to radiological hazards from Ilorin-south kaolin mine field. These radionuclides have been noted for their notorieties and contributions to background ionizing radiation which is linked with various kinds of cancers, liver diseases and ruthless health related harms which could eventually lead to death.

Table 5 Summary of the estimated D_o, D_i, *AED*, *ELCR* and *RLI* for the measured activity concentrations.

LOCATION	STAT	D_o ($nGyh^{-1}$)	AED_{out} ($mSvy^{-1}$)	*ELCR* ($X\ 10^{-3}$)	*RLI*
	MIN	45.92	0.06	0.20	0.71
ILN-WEST	**MAX**	81.92	0.10	0.35	1.32
In situ	**MEAN±STDEV**	63.28±10.48	0.08±0.01	0.27±0.05	1.01±0.17
	MIN	13.90	0.02	0.06	0.23
ILN-SOUTH	**MAX**	88.30	0.11	0.37	1.35
In situ	**MEAN±STDEV**	54.71±16.68	0.07±0.02	0.23±0.07	0.84±0.25
	LIMIT	**59.00**	**0.07**	**3.75**	**≤1**
LOCATION	**STAT**	D_i ($nGyh^{-1}$)	AED_{in} ($mSvy^{-1}$)	*ELCR* ($X\ 10^{-3}$)	*RLI*
	MIN	45.84	0.22	0.79	0.39
ILN-WEST	**MAX**	99.11	0.49	1.70	0.83
	MEAN±STDEV	72.67±16.64	0.36±0.13	1.25±0.36	0.61±0.18
	MIN	38.88	0.19	0.67	0.30
ILN-SOUTH	**MAX**	143.56	0.70	2.46	1.16
	MEAN±STDEV	76.47±18.24	0.38±0.29	1.31±0.44	0.62±0.21
	LIMIT	**84.00**	**0.41**	**3.75**	**≤1**

Table 6 Summary of the estimated H_{ext}, H_{int}, Ra_{eq} and *AGED* for the measured activity concentrations

LOCATION	STAT	H_{ext}	H_{int}	Ra_{eq} ($Bqkg^{-1}$)	*AGED* ($mSvy^{-1}$)
	MIN	0.27	0.32	98.10	0.32
ILN-WEST	MAX	0.48	0.64	175.45	0.59
In situ	MEAN±STDEV	0.37±0.06	0.47±0.09	136.55±23.20	0.45±0.07
	MIN	0.09	0.12	32.61	0.10
ILN-SOUTH	MAX	0.53	0.84	193.49	0.59
In situ	MEAN±STDEV	0.32±0.10	0.46±0.16	117.28±36.25	0.37±0.11
	LIMIT	≤1	≤1	370.00	0.30
LOCATION	**STAT**	H_{ext}	H_{int}	Ra_{eq} ($Bqkg^{-1}$)	*AGED* ($mSvy^{-1}$)
	MIN	0.15	0.18	53.93	0.17
ILN-WEST	MAX	0.32	0.42	117.57	0.36
	MEAN±STDEV	0.23±0.08	0.29±0.09	84.70±21.87	0.27±0.08
	MIN	0.11	0.18	41.87	0.14
ILN-SOUTH	MAX	0.46	0.69	168.31	0.51
	MEAN±STDEV	0.24±0.11	0.36±0.11	88.54±22.41	0.27±0.10
	LIMIT	≤1	≤1	370.00	0.30

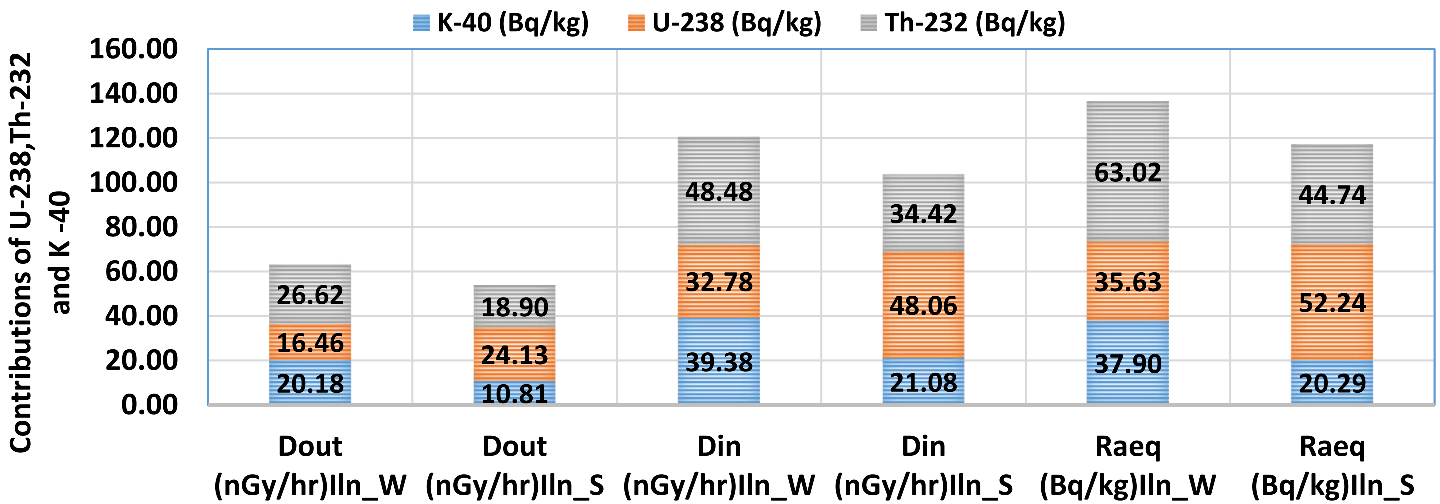

Fig. 10. Contributions of ^{40}K, ^{238}U **and** ^{232}Th *to* D_o, D_i **and** Ra_{eq} **(Iln-W = Ilorin-west and Iln-S = Ilorin-south)**

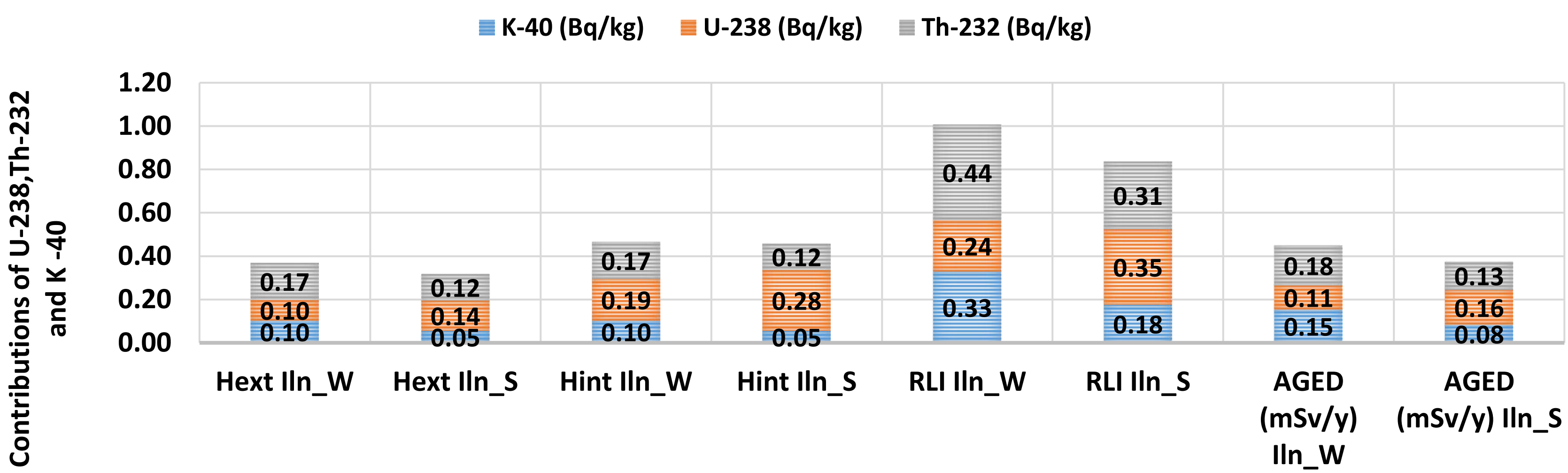

Fig. 11. Contributions of ^{40}K, ^{238}U **and** ^{232}Th *to* H_{ext}, H_{in}, *RLI* **and** *AGED* **(Iln-W = Ilorin-west and Iln-S = Ilorin-south).**

3.4 Monte Carlo Simulation (MCS)

The result of the Monte Carlo simulation performed using Oracle Crystal Ball package version 11.1.2.4.850 for both mining sites is presented in Table 8 and figures 12a – d. The level of risk signifying the 95th percentile, mean, 5th percentile and other level of probability of interest, were determined based on the distribution of the output (Orosun et al., 2020c; Changsheng et al., 2012; Saghi et al., 2019; Orosun, 2021; NRC, 1994; USEPA, 1997). The evaluation of the minimum probable risk (P 5% = best case scenario) reveals that about 167, 104, 706 and 742 individuals in a population of 1 million (10^6) are projected to develop cancer in Ilorin-west (*in-situ*), Ilorin-south (*in-situ*), Ilorin-west (Lab), and Ilorin-south (Lab) respectively. However, the results of the maximum probable risk assessment (P 95% = worst-case scenario) reveals that about 414, 392, 1,900 and 2,460 individuals in a population of 1 million (10^6) are projected to develop cancer in Ilorin-west (*in-situ*), Ilorin-south (*in-situ*), Ilorin-west (Lab), and Ilorin-south (Lab) respectively. Similarly, the most probable risk estimation (50%) reveals that the most likely outcomes are 281, 232, 1,250 and 1,480 individuals in a population of 1 million (10^6) are likely to develop cancer in Ilorin-west (*in-situ*), Ilorin-south (*in-situ*), Ilorin-west (Lab), and Ilorin-south (Lab) respectively. This follows that the mean, P 5% and P 95% cumulative probabilities for the cancer risk for both mining sites are within the recommended value of 3,750.00 x 10^{-6} (UNSCEAR, 2000). Based on the obtained results, there is no substantial environmental or radiological health hazard in the study areas. The results also reveal that inhabitant living around or using the Kaolin from Fufu area of Ilorin-south are the most vulnerable. The outcomes of this research have a potential in order to develop radiation risk assessment models applicable for stakeholders and decision makers for further environmental studies.

Table 8 Summary of the Monte Carlo simulation

	Excess Lifetime Cancer Risk (*ELCR*) (× 10^{-6})		
	5%	Mean (50%)	95%
Ilorin-west (*in-situ*)	167.00	281.00	414.00
Ilorin-south (*in-situ*)	104.00	232.00	392.00
Ilorin-west (Lab)	706.00	1,250.00	1,900.00
Ilorin-south (Lab)	742.00	1,480.00	2,460.00

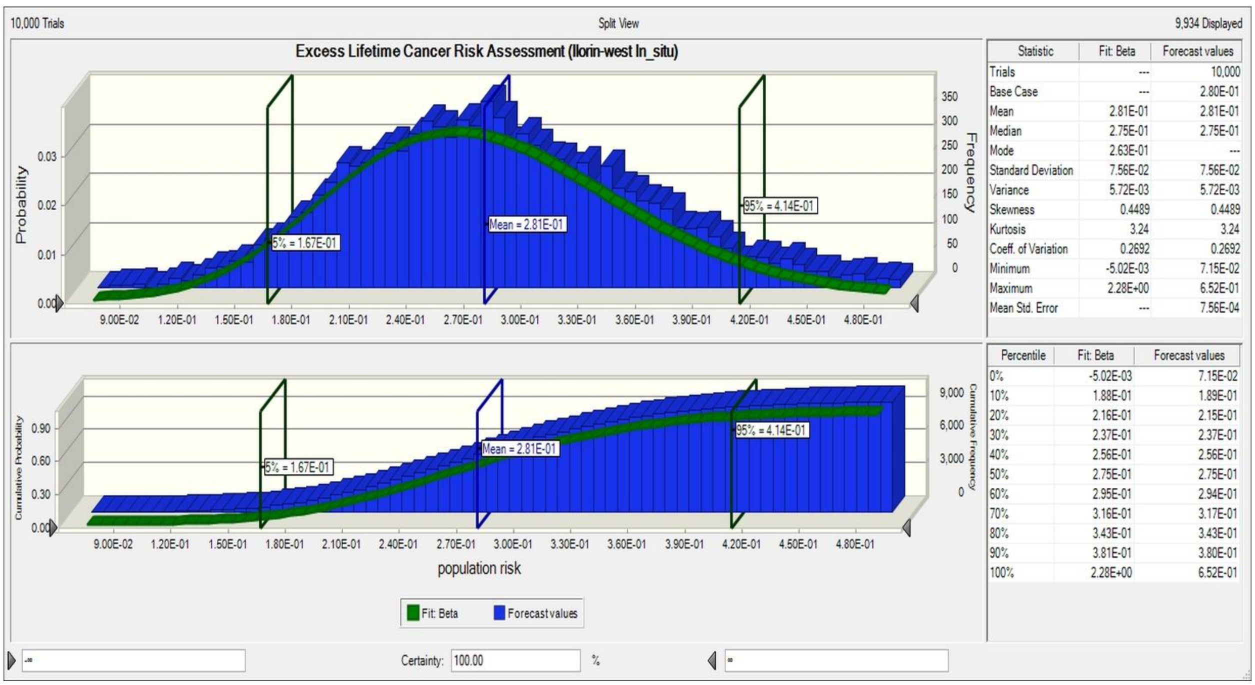

(a) Ilorin-west *in-situ* cancer risk (indicating the mean, P 5% and P 95% cumulative probabilities for the cancer risk)

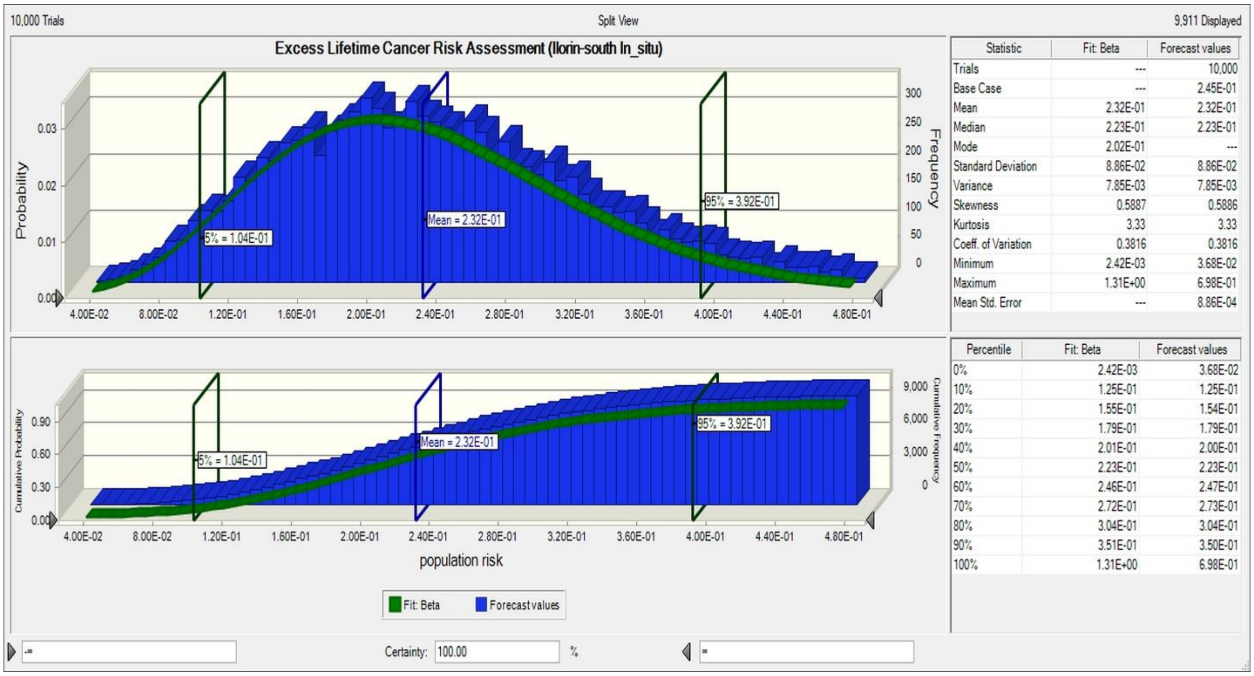

(b) Ilorin-south *in-situ* cancer risk (indicating the mean, P 5% and P 95% cumulative probabilities for the cancer risk)

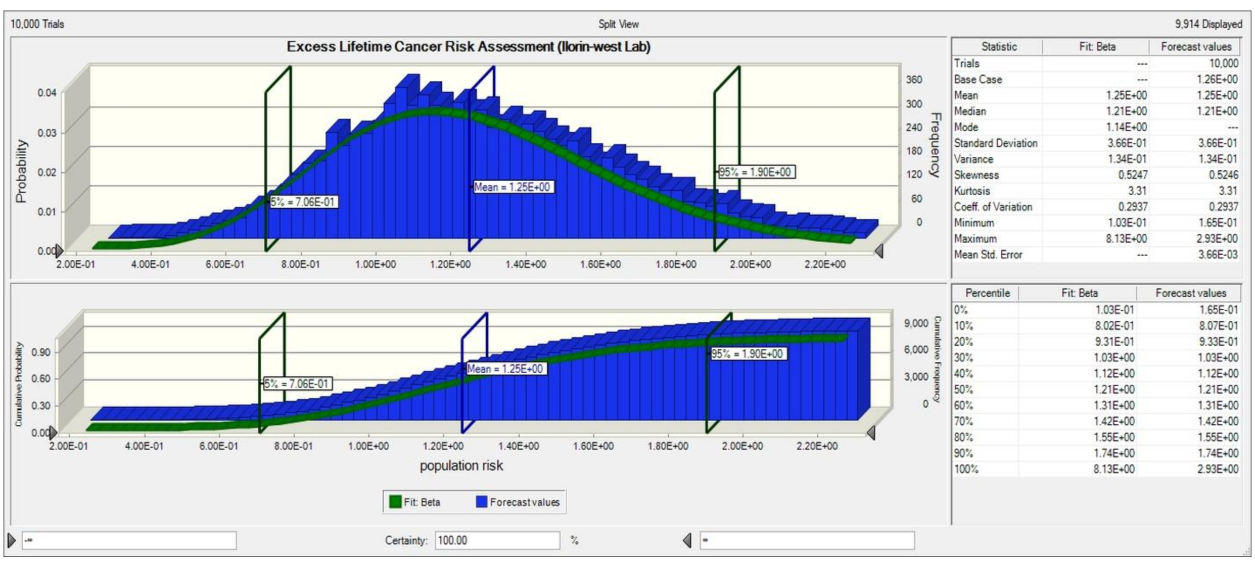

(c) Ilorin-west Lab cancer risk (indicating the mean, P 5% and P 95% cumulative probabilities for the cancer risk)

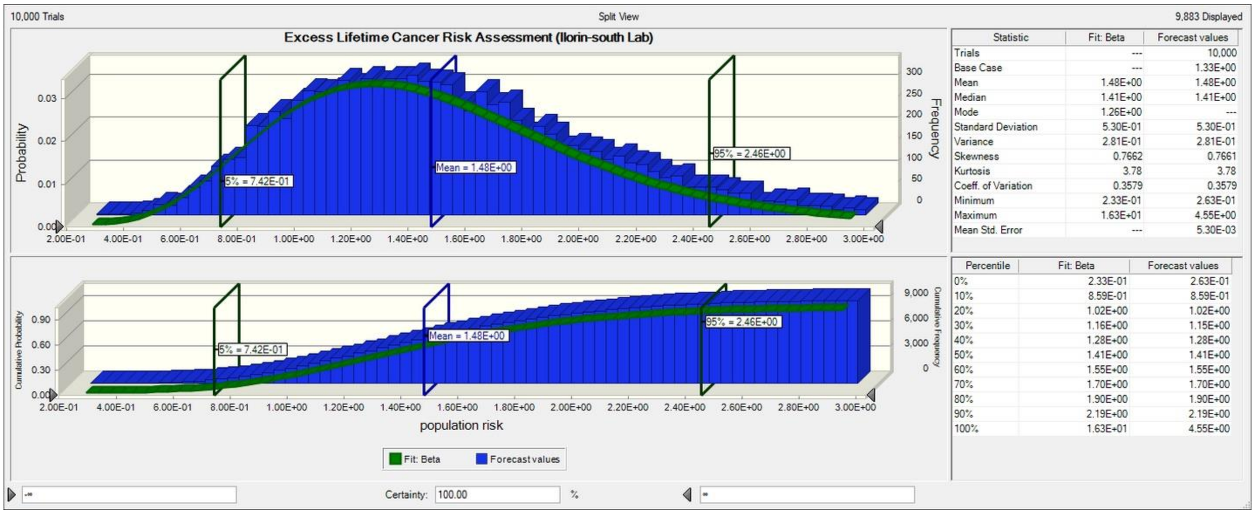

(d) Ilorin-south Lab cancer risk (indicating the mean, P 5% and P 95% cumulative probabilities for the cancer risk)

Figure 12. Cumulative probability plot of the Excess Lifetime Cancer Risk associated with the measured radionuclides at the Kaolin mining sites. (a) Ilorin-west *in-situ* cancer risk, (b) Ilorin-south *in-situ* cancer risk, (c) Ilorin-west Lab cancer risk and (d) Ilorin-south Lab cancer risk.

4. Conclusions

The estimated mean values (both *in situ* and lab results) of ^{40}K, ^{234}Th and *DR* for the Kaolin minefield in Ilorin-west are higher than that of Ilorin-south. However, the mean value of ^{238}U for Ilorin-west is less than the estimated mean value for Ilorin-south. Also, all the measured activity concentrations of ^{40}K, ^{238}U and ^{232}Th in all the locations are lower than their respective *in situ* measurements. The mean values estimated for all radiological parameters for Ilorin-west were comparably higher than that of Ilorin-south mine field for *in situ* measurements. This shows that the Ilorin-west Kaolin mine field poses more significant source of radiation hazard. However, the opposite was the case with the laboratory analysis of the bricks. This unexpected twist was mainly due to the high values of ^{238}U observed in the samples of bricks from Ilorin-south (i.e. the mean concentration of ^{238}U of Ilorin-south is almost twice the mean value obtained for bricks samples from Ilorin-west). The mean values of all the hazard parameters for the bricks from both Ilorin-west and Ilorin-south are less than the recommended limits. The cancer risk assessment using the Monte Carlo simulations reveals values that are mostly within the recommended limits. Therefore, the risk of cancer inducement due to radiation exposure is within the acceptable limits for both mining sites.

Declarations:

- **Conflict of Interests:** The authors declare that they have no conflict of interest.
- **Data availability:** The data supporting the findings of this study are available on request from the corresponding author.
- **Consent for publication:** All authors have read and agreed to the published version of the manuscript.
- **Consent to participate:** Not applicable.
- **Ethics approval:** Not applicable.
- **Animal research:** Not applicable.
- **Funding:** Partial funding which covers survey and laboratory analysis was received via the University of Ilorin Institutional Based Research TETFund program (TETFund IBR). TETFUND/DESS/UNI/ILORIN/2017/RP/VOL.I.

- **Acknowledgement:** The authors acknowledge University of Ilorin Staff Development Award (SDA) for PhD program granted for this research. The support enjoyed from the entire staffs of IBRAJ NIGERIA LIMITED is deeply appreciated.

- **Author contribution:** M.M.O. conceived and designed the research work, performed the Monte Carlo Simulations, and wrote the paper. M.M.O., T.B.A and C.A.O. collect the data, performed the risks analysis and compilation of the work. M.T and M.V contributed to the writing and final editing of the manuscript. M.R.U. and K.J.O. supervised the work and final editing of the manuscript.

References

Adagunodo et al. (2018). Radioactivity and radiological hazards from a kaolin mining field in Ifonyintedo, Nigeria. MethodsX, 5, 362–374.

Ademola, A.K.; Hammed, O.S.; and Adejumobi, C.A. (2008). Radioactivity and dose assessment of marble samples from Igbeti mines, Nigeria. Radiation Protection Dosimetry, 132(1), 94–97. doi:10.1093/rpd/ncn279

Ademola, A.K.; Hammed, O.S.; and Adejumobi, C.A. (2008). Radioactivity and dose assessment of marble samples from Igbeti mines, Nigeria. Radiation Protection Dosimetry, 132(1), 94–97. doi:10.1093/rpd/ncn279.

Ajadi et al. (2016). Effect of effluents discharge on public health in Ilorin Metropolis, Nigeria. Ethiopian Journal of Environmental Studies and Management, 9(4), 389.

Ajayi J.O.; Balogun B.B.; and Olabisi O. (2012). Natural Radionuclide Contents in Raw Materials and the Aggregate Finished Product from Dangote Cement Plc, Obajana, Kogi

State, North Central Nigeria. Research Journal of Environmental and Earth Sciences, 4(11), 959-961, 2012 ISSN: 2041- 0492

Ajibola et al. (2021). Assessment of Annual Effective Dose Associated with Radon in Drinking Water from Gold and Bismuth Mining area of Edu, Kwara, North-central Nigeria, Pollution, 7(1): 231-240.

Akinyose et al. (2018). Radiological Impacts of Natural Radioactivity in Locally Produced Tobacco Products in Ibadan, Oyo State, Nigeria. Momona Ethiopian Journal of Science (MEJS), 10(1), 59-75. http://dx.doi.org/10.4314/mejs.v10i1.5.

Amana M.S. (2017). Radiation hazard index of common imported ceramic using for building materials in Iraq, Aust. J. Basic. Appl. Sci. 11(10), 94–102.

Chandrasekaran et al. (2014). Spatial distribution and life time cancer risk due to gamma radioactivity in Yelagiri Hills,Tamilnadu, India, Egypt. J. Basic Appl. Sci., 1, 38–48.

Changsheng et al. (2012). Monte Carlo Simulation-Based Health Risk Assessment of Heavy Metal Soil Pollution: A Case Study in the Qixia Mining Area, China, Human and Ecological Risk Assessment: An International Journal, 18:4, 733-750. DOI: 10.1080/10807039.2012.688697.

Dailytrust, (2018). “how Nigeria can exploit untapped kaolin deposits”. Available at https://www.dailytrust.com.ng/how-nigeria-can-exploit-untapped-kaolin-deposits-265327.html (Accessed on 22nd February, 2019)

El-Dine et al. (2004). Radioactivity in local and imported kaolin types used in Egypt, Appl. Radiat. Isot., 60, 105–109.

Farai I.P.; and Ademola J.A. (2001). Population dose due to building materials in Ibadan, Nigeria, Radiat.Prot. Dosim. 95, 69-73

IAEA (1996). Radiation protection and the safety of Radiation sources. International Atomic Energy Agency, Wagramerstrsse 5, P. O Box 100, A1400 Vienna, Austria. IAEA-RPSR-1 Rev 1.

IARC (1988) International Agency for Research on Cancer, Monograph on the Evaluation of Carcinogenic Risks to Humans: Man Made Mineral Fibres and Radon, vol. 43. IARC Monograph, Lyon, France. https://publications.iarc.fr/Book-And-Report-Series/Iarc-Monographs-On-The-Identification-Of-Carcinogenic-Hazards-To-Humans/Man-Made-Mineral-Fibres-And-Radon-1988. Accessed 26 January 2021.

ICRP (1991). Recommendations of the International Commission on Radiological Protection 1990 (ICRP) Publication No. 60. Annals of the ICRP 21: 1-201. Elberg. pp119-13.

Isinkaye O.M.; Jibiri N.N.; and Olomide A.A. (2015). Radiological health assessment of natural radioactivity in the vicinity of Obajana cement factory, North Central Nigeria. J Med Phys., 40(1), 52-59.

Isinkaye, O.M. (2018). Distribution and multivariate pollution risks assessment of heavy metals and natural radionuclides around abandoned Iron-ore mines in North Central Nigeria. Earth Systems and Environment, 2, 331–343. doi:10.1007/s41748-018-0035-0.

Janković, B.Ž.; Janković, M.M.; Marinović-Cincović, M.M.; Todorović, D.J; and Sarap, N.B. (2018). Thermal analysis testing and natural radioactivity characterization of kaolin as building material. Journal of Thermal Analysis and Calorimetry, 133(1), 481–487. doi:10.1007/s10973-018-7159-1

Joel et al. (2018a). Assessment of natural radionuclides and its radiological hazards from tiles made in Nigeria. Radiation Physics and Chemistry. 144: 43–47. doi:10.1016/j.radphyschem.2017.11.003.

Kayode et al. (2015). Delineation of the subsurface geological structures of Omu-Aran area, south-western Nigeria, using aeromagnetic data. National Physics Conference 2014 (PERFIK 2014) AIP Conf. Proc., 1657, 040012-1–040012-5. doi: 10.1063/1.4915173.

Leadership (2018). “kaolin as nigerias untapped goldmine” Available at https://leadership.ng/2018/08/15/kaolin-as-nigerias-untapped-goldmine/ (Accessed on 22nd February, 2019)

Mazzilli B.; and Saueia C. (1999). Radiological implications of using phosphogypsum as a building material in Brazil, Radiat. Prot. Dosim., 86 (1), 63–67.

NRC. (1994). Science and Judgment in Risk Assessment. National Research Council. Washington, DC, USA Plum LM, Rink L.

Olusola J.O.; Suraju A.A.; and Nurudeen A. (2013). Geochemical and Mineralogical Studies of Kaolinitic Clays in Parts of Ilorin, Southwestern Basement Rock Area, Nigeria. Universal Journal of Geoscience, 2(7), 212-221.

Omeje et al. (2018). Natural radioactivity concentrations of 226Ra, 232Th, and 40K in commercial building materials and their lifetime cancer risk assessment in Dwellers, Human and Ecological Risk Assessment: An International Journal, 24(8), 2036-2053.

Omeje et al. (2020). Spatial distribution of gamma radiation dose rates from natural radionuclides and its radiological hazards in sediments along river Iju, Ogun state Nigeria. MethodsX. 7: 101086.

Omeje et al. (2021). Measurements of Seasonal Variations of Radioactivity Distributions in Riverine Soil Sediment of Ado-Odo Ota, South-West Nigeria: Probabilistic Approach Using Monte Carlo, Radiation Protection Dosimetry, 2021: ncab027. https://doi.org/10.1093/rpd/ncab027.

Orosun et al. (2017). Natural radionuclide concentration and radiological impact assessment of soil and water from Dadinkowa Dam, Northeast Nigeria. Journal of the Nigerian Association of Mathematical Physics, 42 (1), 307 – 316.

Orosun et al. (2018). Radiological Safety of Water from Hadejia River. IOP Conf. Series: Earth and Environmental Science, 173(2018), 012036 doi:10.1088/1755-1315/173/1/012036.

Orosun et al. (2018b). Measurement of Natural Radionuclides Concentration and Radiological Impact Assessment of Fish Samples from DadinKowa Dam, Gombe State Nigeria. African Journal of Medical Physics, 1(1): 25-35.

Orosun et al. (2019). Natural Radionuclides and Radiological Risk Assessment of Granite Mining Field in Asa,North-central Nigeria, MethodsX. 6, 2504-2514.

Orosun et al. (2020). Dataset on radioactivity measurement of Beryllium mining field in Ifelodun and Gold mining field in Moro, Kwara State, North-central Nigeria, Data in Brief, 31, 105888. https://doi.org/10.1016/j.dib.2020.105888.

Orosun et al. (2020). Radioactivity levels and transfer factor for granite mining field in Asa, North-central Nigeria. Heliyon. 6(6). e04240. https://doi.org/10.1016/j.heliyon.2020.e04240.

Orosun et al. (2020a). Magnetic susceptibility measurement and heavy metal pollution at an automobile station in Ilorin, North-Central Nigeria, Environ. Res. Commun., 2(2020), 015001. https://doi.org/10.1088/2515-7620/ab636a

Orosun et al. (2020c). Monte Carlo approach to risks assessment of heavy metals at automobile spare part and recycling market in Ilorin, Nigeria, Sci. Rep., 10 (2020) 22084. https://doi.org/10.1038/s41598-020-79141-0.

Orosun et al. (2021). Assessment of ambient gamma radiation dose and annual effective dose associated with radon in drinking water from gold and lead mining area of Moro, North-Central Nigeria, Journal of Radioanalytical and Nuclear Chemistry, (2021). https://doi.org/10.1007/s10967-021-07644-9.

Orosun, M. M. (2021). Assessment of Arsenic and Its Associated Health Risks Due to Mining Activities in Parts of North-Central Nigeria: Probabilistic Approach Using Monte Carlo, Journal of Hazardous Materials, 412 (2021): 125262.

Orosun, M. M.; Usikalu, M.R.; Kayode, K. J. (2020b). Radiological hazards assessment of laterite mining field in Ilorin, North-central Nigeria. International Journal of Radiation Research. 18(4), 895-906.

Oyegun, R.O. (1985). The use and waste of water in a third world city. Geo Journal, 10 (2), 205-210.

Oyeyemi et al. (2017). Measurements of radioactivity levels in part of Ota Southwestern Nigeria: Implications for radiological hazards indices and excess lifetime cancer-risks. Journal of Physics: Conference Series, 852, 012042. doi:10.1088/1742-6596/852/1/012042.

Radiation Solution Inc. (2015). RS-125/230 User Manual, Revision 1.05-December 2015, Firmwave Version 5v95, Part Number D-1009, (2015) pp 7.

Saghi et al. (2019). Estimate the effective dose of gamma radiation in Iran cities: lifetime cancer risk by Monte Carlo simulation model. Environmental Geochemistry and Health. 41: 2549–255. doi:10.1007/s10653-019-00300-y.

Turhan, Ş. (2009). Radiological impacts of the usability of clay and kaolin as raw material in manufacturing of structural building materials in Turkey. Journal of Radiological Protection, 29(1), 75–83. doi:10.1088/0952-4746/29/1/005

UNSCEAR (2000). Sources, effects and risks of ionization radiation, United Nations Scientific Committee on the Effects of Atomic Radiation. Report to The General Assembly, with Scientific Annexes B: Exposures from Natural Radiation Sources New York.

USEPA. (1997). Guiding Principles for Monte Carlo Analysis. Washington, DC, USA.

Usikalu et al. (2016). Assessment of geogenic natural radionuclide contents of soil samples collected from Ogun State, South western, Nigeria, International Journal of Radiation Research, 14(3), 355-361.

Usikalu et al. (2017). Assessment of radiological parameters of soil in Kogi State, Nigeria, Environmental Forensics, 18(1), 1-14.

Usikalu et al. (2019). Radiation dose assessment of soil from Ijero Ekiti, Nigeria, Cogent Engineering, 6, 1586271.

Usikalu M.R.; Akinyemi M.L.; and Achuka J.A (2014). Investigation of radiation levels in soil samples collected from selected locations in Ogun State, Nigeria, IERI Procedia, 9, 156-161. DOI: 10.1016/j.ieri.2014.09.056